COBEM 2023 27TH INTERNATIONAL CONGRESS OF MECHANICAL ENGENEERING

ABCM Brazilian Society of Mechanical Sciences and Engineering
27th ABCM International Congress of Mechanical Engineering
December 04-08, 2023, Florianópolis-SC, Brazil

COB-2023-1104
INFLUENCE OF T-STRESS ON THE PROCESSED ZONE AROUND CRACK TIP IN CFRP PLATES

Daniel de Macedo Barreto Netto
PPEMM - Post-Graduate Program in Mechanical Engineering and Materials Technology – CEFET/RJ, Av. Maracanã, 229, RJ,
daniel.netto@aluno.cefet-rj.br

Lucas Lisbôa Vignoli
Center for Technology and Application of Composite Materials, Department of Mechanical Engineering, Federal University of Rio de Janeiro, Macaé, RJ, Brazil
ll.vignoli@mecanica.coppe.ufrj.br

Arthur Adeodato
State University of do Rio de Janeiro – UERJ/IPRJ, Nova Friburgo, RJ, Brazil
arthuradeodato@iprj.uerj.br

Paulo Pedro Kenedi
PPEMM - Post-Graduate Program in Mechanical Engineering and Materials Technology – CEFET/RJ, Av. Maracanã, 229, RJ,
CCGMEC – Mechanical Engineering Department - CEFET/RJ, Av. Maracanã, 229, RJ, Brazil
paulo.kenedi@cefet-rj.br

Abstract. *Carbon fiber reinforced polymer (CFRP) laminates are widely employed in different fields due to their low density combined with high stiffness and strength. However, unlike usual materials, composite laminates may present many different failure mechanisms and the stress distribution depends on the material properties due to its anisotropy. Additionally, unidirectional laminae have a much more severe effect on stress concentrations than isotropic materials. In linear elastic fracture mechanics (LEFM), it is well known that the crack tip has a singularity, and the stress components related to the crack tend to zero far away from the crack tip. Alternatively, the nominal stress influence can be considered through the inclusion of T-stress components. The present investigation aims to analytically evaluate the damaged area around the crack tip, also named the processed zone, with and without the T-stress component. The proposed approach is validated against finite element (FE) simulations using the commercial FE software Ansys in conjunction with the Tsai-Wu failure criterion. The influence of fiber-to-load angle is also studied, carrying out a parametric multiscale analysis and applying the VSPK micromechanical model. The preliminary results indicate that the processed zone increases according to the fiber-to-load angle and the T-stress component becomes relevant for high nominal stress loads.*

Keywords: *processed zone, crack tip, CFRP, Tsai-Wu criterion*

1. INTRODUCTION

In engineering, standard materials can be divided into three major groups: metallic, ceramic, and polymeric (Barbero, 2018). In recent years, composite materials, which are a combination of two or more of these materials, have become more significant. This concept is based on the development of new materials to obtain properties that are better than those of their constituents. The composite material depends not only on the constituents but also on the orientation and the volumetric fraction of how these phases are distributed (Vignoli & Savi, 2018). Composite materials have special advantages over conventional materials such as high mechanical strength, high stiffness, low density, and good corrosion resistance. Modeling the mechanical behavior of a composite material is a complex task because involves the material anisotropy, according to the fiber orientation and distribution (Vignoli *et al*., 2020a).

The knowledge of material properties is an important matter to the design of a structure, but it is also necessary to assess whether the material will fail under a particular stress condition. For isotropic ductile materials, the criteria of Tresca and von Mises are generally used. For composite materials, more complex criteria have been developed, by extending and adapting the isotropic failure theories, to account for the existent anisotropy. For the structural analysis of a laminated composite, after calculating the stresses, it is necessary to evaluate the failure modes and the respective damages to the structure. A structural failure refers to the loss of the ability to perform its function appropriately. There are some different failure modes for composites. According to Agarwal *et al*. (2006), failure can occur because of the fiber, matrix, or delamination.

Using micromechanical arguments, Vignoli *et al*. (2020b) investigated fiber failure in tension and compression, while Vignoli *et al*. (2020c) carried out a study to evaluate different modes of matrix failure. To predict the stress state responsible for these failures, a variety of experiments and failure criteria have been proposed in the literature.

Hill (1948) proposed a theory to describe, on a macroscopic scale, the yielding and plastic flow of anisotropic metals. This work served as the basis for Azzi & Tsai (1965) to develop the well-known Tsai-Hill criterion. Tsai & Wu (1971) also developed a criterion that is now widely used for unidirectional composites. It was derived from a scalar function of two strength tensors, satisfying the conditions given by the invariants to the coordinate transformation. It deals with the interaction terms as independent components. This criterion considers the differences between tensile and compressive strengths. It can be specified for different material symmetry, multidimensional space, and multiaxial loading.

Another criterion was proposed by Hashin (1980), that can distinguish between the different failure modes, modeling each of them separately. Hashin also established a three-dimensional failure criterion for unidirectional composites in terms of quadratic polynomials. It was expressed in terms of the mean stress state invariants for transversely isotropic materials. Four different failure modes (fiber and matrix, tension, and compression modes) were modeled separately. Puck and Schurmann (1998) provided a detailed evaluation of theoretical methods for the initial failure of unidirectional composites.

Hinton & Soden (1998) conducted a study involving several researchers that became known as the World-Wide Failure Exercise (WWFE). WWFE aimed to present a comprehensive description of most of the failure theories available at the time and compare its predictive capabilities with experimental data. According to WWFE results Hinton *et al*. (2004), Tsai-Wu and Puck failure criteria are the most reliable among those compared by the participants, where the Tsai-Wu has the advantage of using one simple polynomial equation.

Even considering these advances in the evaluation of composite damages, there are still limited studies related to the behavior of macromechanical notched composite plates. Concerning a circular hole, Vignoli *et al*. (2019) showed that matrix failure is dominant for damage initiation. This statement was confirmed for damage propagation by numerical simulations (Vignoli & Castro, 2021) and experimentally (Kenedi *et al*., 2022). Erkan *et al*. (2020) pointed out some issues from notched manufacturing processes, considering that these abrupt geometry variations are unavoidable for real structures. A discussion about different geometry variations that induce stress concentration can be found in Zavvar *et al*. (2021). Some authors, like Catalanotti *et al*. (2014) and Furtado *et al*. (2017), use LEFM concepts to estimate notched plate strength. However, the LEFM has some theoretical limitations concerning its applicability due to stress singularity. For metals, this issue was extensively discussed, for instance by Sousa *et al*. (2013), evaluating the plastic zone around the crack tip. For composites, the main contribution in this area was presented by Xin *et al*. (2010) using the Hill criterion and a stress solution developed by Sih *et al*. (1965). For a discussion about fracture in metal laminates, see Wang *et al*. (2022).

This paper deals with an analytical study of the damaged area around a crack tip in a unidirectional single-layered CFRP laminate submitted to uniaxial loading. This damaged area is also expressed as the processed zone. Three different coordinate systems are defined, as shown in Fig.1: the material coordinates, where the CFRP properties are defined and fiber are parallel to x_1; the global coordinates, where the load is parallel to $x_1^{(g)}$and the crack is parallel to $x_2^{(g)}$; and the cylindrical coordinates, where r is the distance from the crack tip to a point and θ is the angle between a point of distance r and $x_2^{(g)}$.

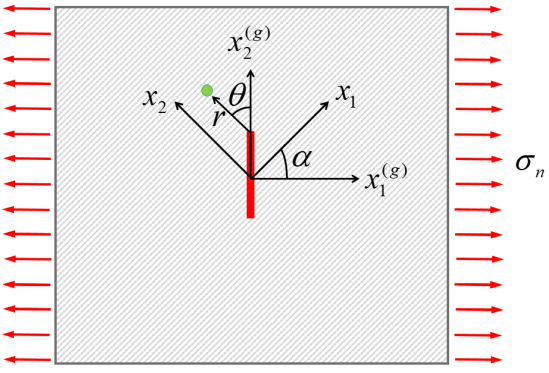

Figure 1. Large CFRP plate with a central crack.

In Section 2, the closed-form analytical equation for the processed zone around the crack tip is derived, considering stress distribution based on LEFM theory and the T-stress component combined with the Tsai-Wu failure criterion. Despite the importance of the T-stress component on the stress field around the crack tip (Castro and Meggiolaro, 2016), it has not been explored in the literature to evaluate the processed zone for anisotropic materials. A numerical model is introduced in Section 3, using the FE method. The results of analytical and numerical approaches are presented and discussed in Section 4 to validate the closed-form equation derived. Final remarks are pointed out in Section 5.

2. CRACK TIP PROCESSED ZONE

Sih *et al*. (1965) proposed that the stress distribution around a crack tip, in a large anisotropic plate, submitted to uniaxial tension, can be written by the following equation, for the plane stress state:

$$\sigma_{ij}^{(g)} = \frac{K_I}{\sqrt{2\pi r}} g_{ij}^{(g)} \tag{1}$$

Where $\sigma_{ij}^{(g)}$ are the stress components with i,j = 1,2, and $K_I = \sigma_n \sqrt{\pi \cdot a}$ is the stress intensity factor in mode I. A central crack, with half-length *a*, perpendicular to the load direction, as presented in Fig. 1, is submitted to the applied nominal stress σ_n. Additionally, $g_{ij}^{(g)}$ are functions defined by:

$$g_{11}^{(g)} = Re\left[\frac{1}{\mu_1-\mu_2}\left(\frac{\mu_1}{\sqrt{\cos\theta+\mu_2\sin\theta}} - \frac{\mu_2}{\sqrt{\cos\theta+\mu_1\sin\theta}}\right)\right] \tag{2}$$

$$g_{22}^{(g)} = Re\left[\frac{\mu_1\mu_2}{\mu_1-\mu_2}\left(\frac{\mu_2}{\sqrt{\cos\theta+\mu_2\sin\theta}} - \frac{\mu_1}{\sqrt{\cos\theta+\mu_1\sin\theta}}\right)\right] \tag{3}$$

$$g_{12}^{(g)} = Re\left[\frac{\mu_1\mu_2}{\mu_1-\mu_2}\left(\frac{1}{\sqrt{\cos\theta+\mu_1\sin\theta}} - \frac{1}{\sqrt{\cos\theta+\mu_2\sin\theta}}\right)\right] \tag{4}$$

Eq. (2-4), *Re* indicates the real part of a complex number, μ_1, and μ_2 are the material eigenvalues computed by roots of the polynomial:

$$S_{22}^{(g)}\mu^4 - 2S_{26}^{(g)}\mu^3 + (2S_{12}^{(g)} + S_{66}^{(g)})\mu^2 - 2S_{16}^{(g)}\mu + S_{11}^{(g)} = 0 \tag{5}$$

where $S_{ij}^{(g)}$ are components of the material compliance matrix in global coordinate. The Eq. (5) roots are always complex numbers, so μ_1 and μ_2 are selected as the roots with positive imaginary parts. The global compliance matrix components can be calculated considering the compliance matrix components in the material coordinate system, S_{ij} and the rotational operation due to the fiber orientation. The compliance matrix components in material coordinates (Barbero, 2018):

$$S_{11} = 1/E_1 \tag{6}$$
$$S_{12} = -\nu_{12}/E_1 \tag{7}$$
$$S_{22} = 1/E_2 \tag{8}$$
$$S_{66} = 1/G_{12} \tag{9}$$

where E_1 is the longitudinal elastic modulus, ν_{12} is the in-plane Poisson's ratio, E_2 is the transversal elastic modulus, and G_{12} is the in-plane shear modulus. Then, $S_{ij}^{(g)}$ can be computed considering the fiber inclination α (Reddy, 2003)

$$S_{11}^{(g)} = S_{11}\cos^4\alpha + (2S_{12} + S_{66})\cos^2\alpha\sin^2\alpha + S_{22}\sin^4\alpha \tag{10}$$
$$S_{12}^{(g)} = S_{12}\cos^4\alpha + (S_{11} + S_{22} - S_{66})\cos^2\alpha\sin^2\alpha + S_{12}\sin^2\alpha \tag{11}$$
$$S_{22}^{(g)} = S_{22}\cos^4\alpha + (2S_{12} + S_{66})\cos^2\alpha\sin^2\alpha + S_{11}\sin^4\alpha \tag{12}$$
$$S_{66}^{(g)} = S_{66}(\cos^2\alpha - \sin^2\alpha)^2 + 4(S_{11} + S_{22} - 2S_{12})\cos^2\alpha\sin^2\alpha \tag{13}$$
$$S_{16}^{(g)} = (2S_{11} - 2S_{12} - S_{66})\cos^3\alpha\sin\alpha + (S_{66} + 2S_{12} - 2S_{22})\cos\alpha\sin^3\alpha \tag{14}$$
$$S_{26}^{(g)} = (2S_{12} - 2S_{22} + S_{66})\cos^3\alpha\sin\alpha + (2S_{11} - 2S_{12} - S_{66})\cos\alpha\sin^3\alpha \tag{15}$$

To include the T-stress component (T), Eq.(1) is rewritten as:

$$\sigma_{ij}^{(g)} = \frac{K_I}{\sqrt{2\pi r}} g_{ij}^{(g)} + T\delta_{i2}\delta_{j2} \tag{16}$$

Nejati *et al*. (2022), propose T-stress for a large anisotropic plate with a central crack submitted to uniaxial load by:

$$T = \sigma_n \,\mathrm{Re}(\mu_1\mu_2) \tag{17}$$

Once the stress distributions in global coordinates are obtained using the equations presented, the damage around the crack tip can be studied. The damaged region around the crack tip, the processed zone, can be evaluated using the Tsai-Wu failure criterion (Tsai & Wu, 1971):

$$f_{TW} = F_1\sigma_{11} + F_2\sigma_{22} + F_{11}{\sigma_{11}}^2 + F_{22}{\sigma_{22}}^2 + F_{66}{\sigma_{12}}^2 + F_{12}\sigma_{11}\sigma_{22} \tag{18}$$

where σ_{ij} are the stress components considering the material coordinate system and the strength parameters F_i and F_{ij} are defined by:

$$F_1 = \left(\frac{1}{S_{11}^c} - \frac{1}{S_{11}^t}\right) \tag{19}$$

$$F_2 = \left(\frac{1}{S_{22}^c} - \frac{1}{S_{22}^t}\right) \tag{20}$$

$$F_{11} = \frac{1}{S_{11}^t S_{11}^c} \tag{21}$$

$$F_{22} = \frac{1}{S_{22}^t S_{22}^c} \tag{22}$$

$$F_{66} = \left(\frac{1}{S_{12}^s}\right)^2 \tag{23}$$

$$F_{12} = -\frac{1}{\sqrt{S_{11}^t S_{11}^c S_{22}^t S_{22}^c}} \tag{24}$$

In Eq.(19-24), S_{11}^t is the longitudinal tensile strength, S_{11}^c is the longitudinal compressive strength, S_{22}^t is the transversal tensile strength, S_{22}^c is the transversal compressive strength, and S_{12}^s is the in-plane shear strength.

Note that the stress components in Eq. (16) are defined in global coordinates, while the stress components presented in Eq. (18), for the Tsai-Wu failure criterion, are in material coordinates. Hence, the stress tensor rotation must be carried out using the following operation:

$$\sigma_{ij} = \lambda_{im}\lambda_{jn}\sigma_{mn}^{(g)} \tag{25}$$

where is the rotational operator (Sokolnikoff, 1956).

The processed zone is the region where $f_{TW} \geq 1$. The border of this region can be obtained considering that $r = r_P$. Hence,

$$\left(\frac{K_I}{\sqrt{2\pi r_P}}\right)^2 \left({h_{11}}^2 F_{11} + {h_{22}}^2 F_{22} + {h_{12}}^2 F_{66} + h_{11}h_{22}F_{12}\right) + \frac{K_I}{\sqrt{2\pi r_P}}\left(h_{11}F_1 + h_{22}F_2\right) = 1 \tag{26}$$

where

$$h_{11} = g_{11}^{(g)}\cos^2\theta + g_{22}^{(g)}\sin^2\theta + 2g_{12}^{(g)}\sin\theta\cos\theta \tag{27}$$

$$h_{22} = g_{11}^{(g)}\sin^2\theta + g_{22}^{(g)}\cos^2\theta - 2g_{12}^{(g)}\sin\theta\cos\theta \tag{28}$$

$$h_{12} = -g_{11}^{(g)}\sin\theta\cos\theta + g_{22}^{(g)}\sin\theta\cos\theta + 2g_{12}^{(g)}(\cos^2\theta - \sin^2\theta) \tag{29}$$

Eq. (26) can be solved analytically, and the following closed-form equation can be achieved:

$$r_P = \frac{a}{2}\left[\frac{2({h_{11}}^2 F_{11} + {h_{22}}^2 F_{22} + {h_{12}}^2 F_{66} + h_{11}h_{22}F_{12})}{-(h_{11}F_1 + h_{22}F_2) + \sqrt{(h_{11}F_1 + h_{22}F_2)^2 + 4({h_{11}}^2 F_{11} + {h_{22}}^2 F_{22} + {h_{12}}^2 F_{66} + h_{11}h_{22}F_{12})}}\sigma_n\right]^2 \tag{30}$$

3. FINITE ELEMENT MODEL

The present FE model is developed using the commercial software Ansys 2022R1. Fig. 2a presents a schematic representation of the boundary conditions and geometry. To obtain a uniform uniaxial load, a displacement is applied, and the resultant load is computed by the force reaction. The plate geometry has a square shape with a length equal to 1200 mm and thickness equal to 1 mm, assuming the plane stress state. The crack is represented as an elliptical hole with major and minor semi-axes equal to 10 mm and 0.01 mm, respectively. The plate and crack geometries are defined based on Góes *et al*. (2014), where the authors suggest that an elliptical hole can be used to represent the crack to avoid singularities in the stress field, improving the simulation convergence.

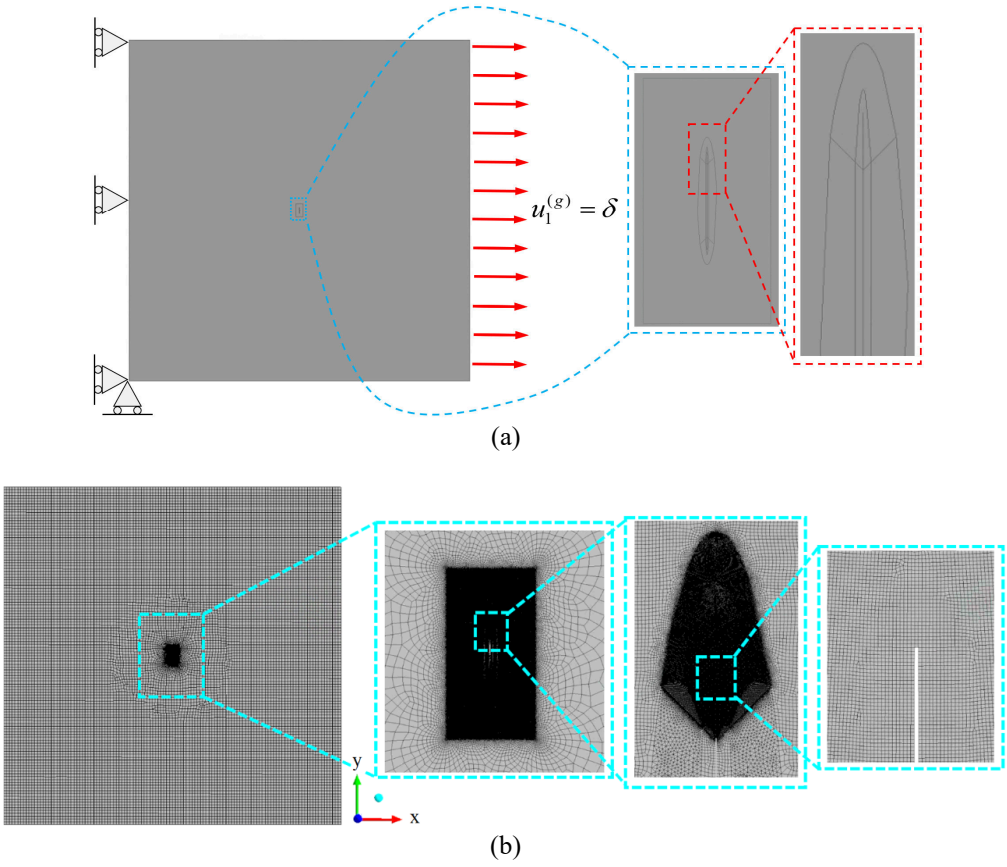

Figure 2. FE model: (a) applied boundary conditions; (b) convergence mesh.

To improve the mesh generation, the plate is split near the crack. First, a rectangular area is created with horizontal and vertical lengths equal to 26 mm and 50 mm, respectively. Two additional ellipses are added around the crack, the first one with a semi-axis of 13 mm and 2 mm and the second one with an axis of 11 mm and 0.5 mm. At last, these ellipses are split around the crack tip with lines distant 2.5 mm from the crack tip and oriented at 45º. The convergence FE mesh is represented in Fig. 2b.

The quadratic element PLANE183 is used to achieve mesh convergence, resulting in 368585 elements and 1092105 nodes. The finest element size is 0.001 mm, and it is defined in the region closest to the crack tip, while the elements far from the crack tip have sizes up to 10 mm.

4. RESULTS AND DISCUSSIONS

An IM7/8552 CFRP plate made by IM7 fiber and 8552 epoxy matrix is selected to implement the analytical and numerical models. The following properties are considered Tsai & Melo (2017): $E_1 = 159\,\text{GPa}$, $E_2 = 8.96\,\text{GPa}$, $G_{12} = 5.5\text{GPa}$, $\nu_{12} = 0.32$, $S_{11}^t = 2501\,\text{MPa}$, $S_{11}^c = 1700\,\text{MPa}$, $S_{22}^t = 64\,\text{MPa}$, $S_{22}^c = 2501\,\text{MPa}$, $S_{12}^s = 120\,\text{MPa}$. Fig. 3 shows the processed zones $\alpha = 0°,45°,90°$.

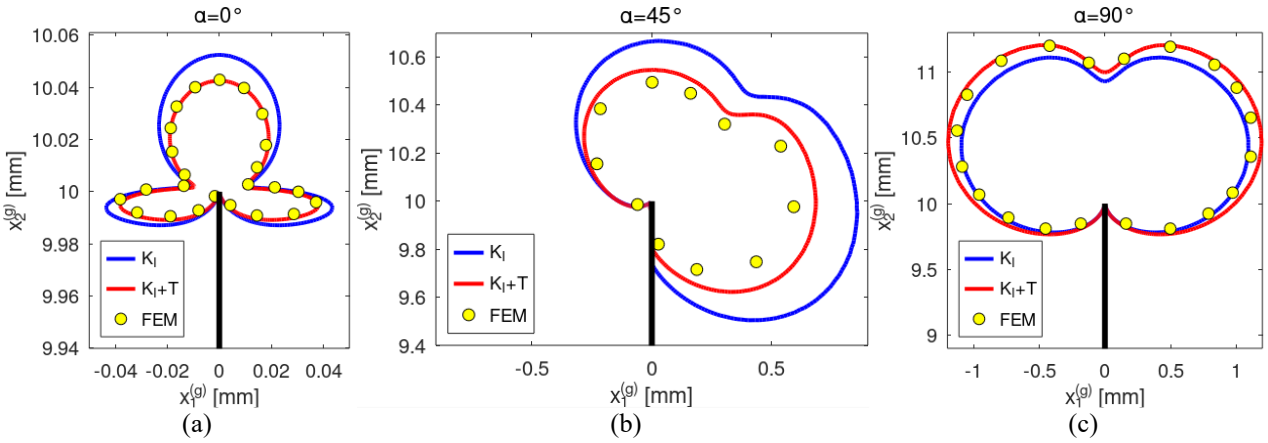

Figure 3. Comparison between processed from analytical models without (K_I) and with T-stress (K_I+T) and FE simulations, for: (a) α = 0º, (b) α = 45º, and (c) α = 90º.

The results indicate a very good estimation of the proposed analytical modeling approach. The model with the T-stress component obtained the best results, when compared with the model without considering the T-stress component, using the FE model as a reference.

5. CONCLUSIONS

This paper studies the influence of the T-stress component on the processed zone around the crack tip for a CFRP submitted to uniaxial loading. An analytical model is derived to obtain the closed-form equation of the processed zone border-radius. The estimations are compared with an FE simulation, indicating a very good agreement and, therefore, reassuring the importance of utilizing the T-stress approach.

6. ACKNOWLEDGEMENTS

The authors would like to acknowledge the support of the Brazilian Research Agency FAPERJ.

7. REFERENCES

Agarwal, B.D., Broutman, L.J., Chandrashekhara, K., 2006. "Analysis and Performance of Fiber Composites", Wiley, USA.

Azzi, V.D., Tsai, S.W., 1965. "Anisotropic Strength of Composites", *Experimental Mechanics*, Vol. 5, pp. 283-288.

Barbero, E.J., 2018. "Introduction to composite materials design", 3rd edition, CRC Press, USA.

Castro, J.T..P, Meggiolaro, M.A., 2016. "Fatigue Design Techniques, Volume 3: Crack Propagation, Temperature, and Statistical Effects", 1st edition, Scotts Valley, CA 95066, USA: CreateSpace.

Catalanotti, G., Arteiro, A., Hayati, M., Camanho, P.P., 2014. "Determination of the mode I crack resistance curve of polymer composites using the size-effect law", *Engineering Fracture Mechanics*, Vol. 118, pp. 49-65.

Erkan, O., Sur, G., Nas, E., 2020. "Investigation of Surface Morphology of Drilled CFRP Plates and Optimization of Cutting Parameters", Surface Review and Letters, Vol. 27, pp. 1950209.

Furtado, C., Arteiro, A., Bessa, M.A., Wardle, B.L., Camanho, P.P., 2017. "Prediction of size effects in open-hole laminates using only Young's modulus, the strength, and the R-curve of the 0° ply", *Composites Part A: Applied Science and Manufacturing*, Vol. 101, pp. 306-317.

Góes, R.C.O., Castro, J.T.P., Martha, L.F., (2014), "3D effects around notch and crack tips", *International Journal of Fatigue*, Vol. 62, pp. 159-170.

Kenedi, P.P., Vignoli, L.L., Duarte, B.T., Silva Neto, J.S.E, Bandeira, C.F.C., 2022. "Damage tracking of notched composite plates by thermography: Experimental observations and analytical model for damage onset", *Journal of Composite Materials*, Vol. 56, pp. 1211-1220.

Hashin, Z., 1980. "Failure Criteria for Unidirectional Fiber Composites", *Journal of Applied Mechanics*, Vol. 47, pp. 329-334.

Hill, R., 1948. "A theory of the yielding and plastic flow of anisotropic metals", *Proc. R. Soc. Lond. A*, Vol. 193, pp. 281–297.

Hinton, M.J., Kaddour, A.S., Soden, P.D., 2004. "Failure Criteria in Fibre-Reinforced-Polymer Composites - The World-Wide Failure Exercise", Elsevier.

Hinton, M.J., Soden, P.D., 1998. "Predicting failure in composite laminates: the background to the exercise", *Composites Science and Technology*, Vol. 58, pp. 1001-1010.

Nejati, M., Ghouli, S., Ayatollahi, M.R., 2022. "Crack tip asymptotic fields in anisotropic planes: Importance of higher order terms", *Applied Mathematical Modelling*, Vol. 91, pp. 837–862.

Puck, A., Schurmann, H., 1998. "Failure analysis of FRP laminates using physically based phenomenological models", *Composites Science Technology*, Vol. 58, pp. 1045–1067.

Reddy, J.N., 2003. "Mechanics of laminated composite plates and shells: theory and analysis", 2nd edition, CRC press.

Sih, G.C., Paris, P.C., Irwin, G.R., 1965. "On cracks in rectilinearly anisotropic bodies", *International Journal of Fracture Mechanics*, Vol. 1, pp. 189–203.

Sokolnikoff, I.S., 1956. "Mathematical theory of elasticity", 2nd edition, McGraw-Hill Book Company, New York.

Sousa, R.A., Castro, J.T.P., Lopes, A.A.O., Martha, L.F., 2013. "On improved crack tip plastic zone estimates based on T-stress and complete stress fields", *Fatigue & Fracture of Engineering Materials & Structures (Print)*, Vol. 36, pp. 25-38.

Tsai, S.W., Wu, E.M., 1971. "A general theory of strength for anisotropic materials", *J. Compos. Mater.*, Vol. 5, pp. 58-80.

Vignoli, L.L., Castro, J.T.P., 2021. "A parametric study of stress concentration issues in unidirectional laminates", *Mechanics of Advanced Materials and Structures*, Vol. 28, pp. 1554-1569.

Vignoli, L.L., Castro, J.T.P., Meggiolaro, M.A., 2019. "Stress concentration issues in unidirectional laminates", *Journal of the Brazilian Society of Mechanical Sciences and Engineering*, Vol. 41, pp. 1-27.

Vignoli, L.L., Savi, M.A., 2018. "Multiscale failure analysis of cylindrical composite pressure vessel: a parametric study", *Latin American Journal of Solids and Structures*, Vol. pp. 15, 63.

Vignoli, L.L., Savi, M.A., Pacheco, P.M.C.L., Kalamkaroov, A.L., 2020a. "Multiscale approach to predict the strength of notched composite plates", *Composite Structures*, Vol. 253, pp. 112827.

Vignoli, L.L., Savi, M.A., Pacheco, P.M.C.L., Kalamkaroov, A.L., 2020b. "Micromechanical analysis of longitudinal and shear strength of composite laminae", *Journal of Composite Materials*, Vol. 54, pp. 4853-4873.

Vignoli, L.L., Savi, M.A., Pacheco, P.M.C.L., Kalamkaroov, A.L., 2020c. "Micromechanical analysis of transversal strength of composite laminae", *Composite Structures*, Vol. 250, pp. 112546.

Wang, Y., Tayyebi, M., Assari, A., 2022. "Fracture toughness, wear, and microstructure properties of aluminum/titanium/steel multi-laminated composites produced by cross-accumulative roll-bonding process", *Archives of Civil and Mechanical Engineering*, Vol. 22, pp. 49.

Xin, G., Hangong, W., Xingwu, K., Liangzhou, J., 2010. "Analytic solutions to crack tip plastic zone under various loading conditions", *European Journal of Mechanics A/Solids*, Vol. 29, pp. 738-745.

Zavvar, E., Hosseini, A.S., Lotfollahi-Yaghin, M.A., 2021. "Stress concentration factors in steel tubular KT-connections with FRP-Wrapping under bending moments", *Structures*, Vol. 33, pp. 4743-4765.

8. RESPONSIBILITY NOTICE

The authors are the only ones responsible for the printed material included in this paper.